Network analysis of U.S. non-fatal opioid-involved overdose journeys, 2018–2023

Lucas H. McCabe[1,2*], Naoki Masuda[3,4*], Shannon Casillas[5], Nathan Danneman[1], Alen Alic[5] and Royal Law[5]

*Correspondence:
lucasmccabe@gwu.edu;
naokimas@buffalo.edu

[1] LMI, 7940 Jones Branch Drive, Tysons, VA 22102, USA
[2] Department of Computer Science, The George Washington University, 800 22nd Street NW, Washington, DC 20052, USA
[3] Department of Mathematics, State University of New York at Buffalo, 244 Mathematics Building, Buffalo, NY 14260, USA
[4] Institute for Artificial Intelligence and Data Science, State University of New York at Buffalo, 215 Lockwood Hall, Buffalo, NY 14260, USA
[5] National Center for Injury Prevention and Control, Centers for Disease Control and Prevention, 4770 Buford Highway, NE, Atlanta, GA 30341, USA

Abstract

We present a nation-wide network analysis of non-fatal opioid-involved overdose journeys in the United States. Leveraging a unique proprietary dataset of Emergency Medical Services incidents, we construct a journey-to-overdose geospatial network capturing nearly half a million opioid-involved overdose events spanning 2018–2023. We analyze the structure and sociological profiles of the nodes, which are counties or their equivalents, characterize the distribution of overdose journey lengths, and investigate changes in the journey network between 2018 and 2023. Our findings include that authority and hub nodes identified by the HITS algorithm tend to be located in urban areas and involved in overdose journeys with particularly long geographical distances.

Keywords: Opioid overdoses, Geospatial networks, Transportation networks, Public health, Emergency medical services, HITS algorithm

Introduction

The toll of the drug overdose epidemic in the United States is staggering. More than one hundred thousand people lost their life from a drug overdose in 2021 alone (Spencer et al. 2022b). Opioids have been a major driver of the epidemic, and opioid overdose mortality in the U.S. has grown exponentially since 1979 (Jalal et al. 2018). Furthermore, the rate of nonfatal drug overdose Emergency Medical Services (EMS) encounters involving opioids nearly doubled from January 2018 to March 2022 (Casillas et al. 2022). Evidence suggests that state-level efforts have been moderately successful in reducing misuse of prescription opioids (Dart et al. 2015), but such policies may have unintentionally increased opioid mortality by indirectly incentivizing illicit usage (Lee et al. 2021). For every fatal drug overdose there are many more nonfatal overdoses, and EMS data uniquely provide information on where nonfatal overdoses occur, as well as details on patient residence. This information can be used for understanding how far from a person's place of residence they experienced an overdose, hereafter called a journey to overdose.

Network analysis has been proven to be useful for studying multiple types of public health questions, including disease transmission, diffusion of health-related behavior and information, and social support networks, which are relevant to opioid overdose (Luke

and Harris 2007; Luke and Stamatakis 2012; Valente and Pitts 2017). In the context of the opioid overdose crisis, social network analysis of Appalachians found that over half the individuals in their data set had a first-degree relationship with someone who experienced an opioid overdose, and this proportion was higher near city centers (Rudolph et al. 2019). It was also found that measures of network centrality and prominence can elucidate illicit opioid-seeking behavior (Perry et al. 2019; Yang et al. 2022).

The journey to overdose stems from the so-called "journey to crime," a framework for conceptualizing mobility patterns in environmental criminology. Typically, each event is associated with an origin (e.g., home), destination (e.g., site of the offence), and intermediate phase, wherein an individual is assumed to have traveled from the origin to the destination (Rengert 2002), indicating that network science tools may be appropriate for such analyses. Although journey-to-crime distances are often fairly short (Phillips 1980), recent work has identified offense and offender categories for which journey-to-crime distances tend to be longer (Vandeviver et al. 2015; Van Daele and Vander Beken 2010; Chen and Lu 2021), suggesting that long journeys may be worth examining in their own right.

To the best of our knowledge, Oser et al. applied the concept of geographical discordance to drug overdoses for the first time (Oser and Harp 2015). They found that people who use drugs who traveled to counties other than those of their residences for substance abuse treatment are more likely to relapse with prescription opioids. They also found that geographically discordant treatment efforts (i.e., when those in treatment obtain it in a county other than that of their residence) are more common among rural populations than suburban or urban ones. Johnson et al. studied trip distance to drug purchase arrest for several classes of controlled substances, leveraging arrest record data from Camden, New Jersey. They showed that race and ethnicity were significantly correlated with trip distance, underscoring the relationship between geospatial segregation and drug purchase patterns (Johnson et al. 2013). Donnelly et al. examined trips leading to opioid possession arrest in Delaware, finding dependency of journey length on age, gender, and racial covariates (Donnelly et al. 2021). Forati et al. applied spatial network methods to analyze geographically discordant opioid overdoses, i.e., those that occur in locations distinct from the residence of the person who experienced the overdose. Their work, which concerned fatal incidents in Milwaukee, Wisconsin between 2017 and 2020, was the first to analyze an overdose journey network (Forati et al. 2023). However, the trips quantified in these studies were relatively short, and the study included only a single area. In the present study, we extend these works to a larger spatial scale (i.e., across the U.S.) and to a time horizon that includes the COVID-19 pandemic.

Materials and methods

Data

This section introduces data and several domain-specific acronyms that may not be familiar to all audiences. The acronyms are itemized in Table 4 for readers' convenience.

EMS data

We utilize a proprietary dataset sourced from biospatial, Inc., a platform specializing in the collection and analysis of EMS data (biospatial 2023). Company biospatial aggregates

information from hundreds of counties across 42 U.S. states, including 27 with full coverage and 15 with partial coverage. "Full coverage" states are those from which biospatial receives all records from the state EMS office, while "partial coverage" states provide a subset of the data, sometimes garnered through direct partnerships with EMS providers. Place-of-residence information is collected from the patient, patient's history, or from the EMS destination (e.g., hospital). Data from EMS providers are available at the patient level, but exact information on overdose location and patient residence are not available to external researchers due to privacy protections. We obtain from biospatial a version of the dataset that has been spatially aggregated to protect patient identities. We have visibility of overdose incident locations and patient residences in terms of their encompassing counties or county equivalents (for simplicity, we also refer to them as counties in the following text). We represent counties by their corresponding Federal Information Processing Standards (FIPS) codes, which are five-digit numeric codes assigned by the National Institute of Standards and Technology (NIST) to uniquely represent counties within the U.S.

The Council of State and Territorial Epidemiologists (CSTE) is a U.S. non-profit public health organization providing the Nonfatal Opioid Overdose Standard Guidance, a procedure for identifying suspected opioid-involved overdose encounters by querying coded data elements and patient care report narratives. Specifically, it considers provider impressions, symptoms observed, medications administered and the subsequent response, and keywords considered opioid-related or overdose-related. Following this protocol, we sub-set our data to nonfatal opioid occurrences and remove request cancellations and EMS call-outs coded as assisting another primary agency (Council of State and Territorial Epidemiologists 2022).

Coverage and completeness of biospatial's EMS data vary by time period and reporting agency. Company biospatial maintains an internal probabilistic model, based on population characteristics and historical data, that calculates an Underlying Event Coverage (UEC) metric. UEC estimates the portion of total EMS events during a given time period in a county that are captured by the biospatial platform. Therefore, our first exclusion criterion is counties without sufficient data. Following Casillas et al., we only include counties with a UEC of at least 75% during each quarter of the study period, in part to mitigate bias associated with under-reporting (Casillas et al. 2022). We briefly assess robustness of the results of the downstream analysis with respect to this threshold in Sect. "Sensitivity to the UEC threshold". Our second exclusion criterion includes counties that do not share Patient Care Report Narratives with biospatial, limiting the ability of the CSTE opioid overdose definition queries to identify encounters. Lastly, we excluded fatal opioid occurrences and focused on non-fatal opioid-involved overdose encounters. The geographical distribution of event coverage in the dataset is shown in Fig. 6.

Other data

We obtain demographic and socioeconomic statistics from the American Community Survey 2017–2021 5-year Data Release (ACS). The ACS is an annual demographic survey managed by the U.S. Census Bureau, which provides details on education, employment,

housing, and other demographic factors. The survey samples approximately 3.5 million addresses from across the U.S. annually (Bureau 2021).

We also use urbanicity data from the 2013 National Center for Health Statistics (NCHS) Urban-Rural Classification Scheme for Counties (URCS), which categorizes U.S. counties into the following six groups based on urbanization:

- *Large central metro* counties that (i) are in a metropolitan statistical area (MSA) with at least one million residents, (ii) contain the entirety of the MSA's largest principal city, and (iii) are exclusively populated within the MSA's largest principal city or represent at least 250000 inhabitants in one of the MSA's principal cities,
- *Large fringe metro* counties in an MSA that have at least one million residents and are not classified as large central metro. These counties are, for example, the suburbs of large central metros,
- *Medium metro* counties in an MSA with between 250000 and 999999 residents,
- *Small metro* counties in an MSA with fewer than 250000 residents,
- *Micropolitan* counties in micropolitan statistical areas, and
- *Noncore* counties in neither MSAs nor micropolitan statistical areas (Ingram and Franco 2014).

As in Casillas et al. (2022), we refer to large central metropolitan, large fringe metropolitan, medium metropolitan, or small metropolitan counties as being urban, and micropolitan and noncore counties as being rural, for simplicity. We also provide results for all six categories in Appendix "County profiles with uncollapsed urbanization categories".

The U.S. Census maintains the Topologically Integrated Geographic Encoding and Referencing (TIGER) system (Service 2023), which provides cartographic information about U.S. geographic areas. We extract county boundary coordinates from TIGER's shape files to support our analysis of overdose journey distances.

Construction of a nationwide spatial network of overdose journeys

Using EMS event records spanning January 2018 to March 2023, we construct a nationwide geospatial network from nonfatal opioid-involved overdose events. We aggregated the data on a semiannual basis, with each period representing six consecutive months and the first period of each year consisting of January through June. Each node of the network represents a county with a corresponding FIPS code. A directed edge (u, v) signifies an overdose journey from county u to county v, and its edge weight represents the number of opioid-involved overdose events having occurred in county v, involving people who experienced an overdose residing in county u. Self-loops are edges where the source and destination counties are the same (i.e., $u = v$). Edges that are not self-loops represent geographically discordant overdose events (Forati et al. 2023). We show in Fig. 1 the journey network after applying our exclusion criteria.

Measures of networks

Degree

The weighted in-degree of node v is defined as the number of overdose events that originate from any other node and occur in node v. Similarly, the weighted out-degree
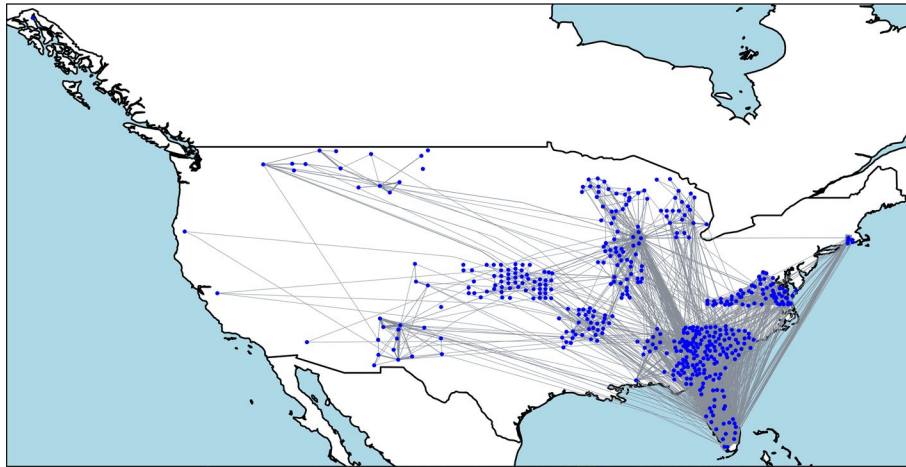
Fig. 1 Visualization of the network of overdose journeys laid over a U.S. map. For visual clarity, the edge widths shown are proportional to the square root of the true edge weights. Self-loops and edge directionality are omitted

of node v is the number of overdose events originating from v and occurring in a different node. In other words, the weighted in- and out-degree reflects the total number of overdose events imported from or exported to other counties. The unweighted in-degree of node v is the number of other nodes for which an overdose event originates and occurs in node v, that is, the number of distinct counties of residence for people who experienced an overdose event occurring in v. The unweighted out-degree of node v is the number of other nodes for which an overdose event originates in node v.

Reciprocity of directed edges

We measure the reciprocity of edges, denoted by r, which quantifies the tendency for nodes in a directed network to form mutual connections (Newman et al. 2002; Garlaschelli and Loffredo 2004; Newman 2018). It is defined by

$$r = \frac{\sum_{i=1}^{N} \sum_{j=1}^{N} A_{ij} A_{ji}}{\sum_{i=1}^{N} \sum_{j=1}^{N} A_{ij}}, \tag{1}$$

where N is the number of nodes, and $A = (A_{ij})$ is the unweighted adjacency matrix such that $A_{ij} = 1$ if there is an edge from the ith to the jth node, and $A_{ij} = 0$ otherwise. The numerator of Eq. (1) counts the number of reciprocal (i.e., bidirectional) edges, and the denominator counts the total number of directed edges in the network. The reciprocity ranges between 0 and 1.

Hyperlink-induced topic search

Hyperlink-Induced Topic Search (HITS), originally proposed in web analytics, ranks nodes in a directed network with respect to their roles as *hubs* or *authorities* (Kleinberg 1999). By definition, a hub is a node that tends to send outgoing edges to authority nodes, while an authority is a node that tends to receive incoming edges from hubs.

A hub and authority are, at first glance, conceptually similar to nodes with a high out-degree and in-degree, respectively. However, a hub, for example, is different from a node with a high out-degree in that an ith node should send many outgoing edges to authority nodes, not ordinary nodes, for the ith node to become a strong hub.

The HITS algorithm assigns each ith node a hub score, denoted by $h(i)$, and an authority score, denoted by $a(i)$. These scores are initialized to 1 and follow an iterative update-normalize algorithm. A single updating round of the hub and authority score invokes the following formulae:

$$h(i) = \sum_{j \text{ such that } j \leftarrow i} a(j), \tag{2}$$

$$a(i) = \sum_{j \text{ such that } j \rightarrow i} h(j), \tag{3}$$

after which we divide each $h(i)$ by $\sqrt{\sum_{j=1}^{N} h(j)^2}$ and each $a(i)$ by $\sqrt{\sum_{j=1}^{N} a(j)^2}$ for normalization. We repeat these steps (i.e., Eqs. (2) and (3), followed by the normalization) until all $h(i)$ and $a(i)$ sufficiently converge.

The hub score $h(i)$ quantifies the extent to which a node serves as a good "recommender" of other nodes, aggregating the authority scores of the nodes to which the ith node points. Conversely, the authority score $a(i)$ aggregates the hub scores of all nodes pointing to i. By identifying hubs and authorities, i.e., nodes with high hub and authority scores, respectively, we aim to identify counties that are pivotal in the spatial distribution of opioid-involved overdoses, as was done in a previous study on overdose journeys (Forati et al. 2023). Hub counties are interpreted to be focal exporters of opioid-involved overdose events, and authority counties are focal importers.

Edge persistence

In temporal networks represented by a time series of static networks in discrete time, edge persistence is the tendency for edges present at one time to be present in the subsequent time. We measure edge persistence by the temporal correlation coefficient (Clauset and Eagle 2007; Tang et al. 2010; Nicosia et al. 2013; Masuda and Lambiotte 2020). The usual formulation of the temporal correlation coefficient for the ith node, denoted by γ_i, is given by

$$\gamma_i = \frac{1}{T-1} \sum_{t=1}^{T-1} \frac{\sum_{j=1}^{N} A_{ij}(t) A_{ij}(t+1)}{\sqrt{\left(\sum_{j=1}^{N} A_{ij}(t) \right) \left(\sum_{j=1}^{N} A_{ij}(t+1) \right)}}, \tag{4}$$

where N is the number of nodes in the temporal network, T is the number of discrete time points, and $A(t)$ represents the $N \times N$ undirected adjacency matrix at time t, with $A_{ij}(t) \in \{0, 1\}$. The network's overall temporal correlation coefficient is given by

$$\gamma = \frac{1}{N} \sum_{i=1}^{N} \gamma_i. \tag{5}$$

As pointed out in Büttner et al. (2016), Eq. (4) treats incoming edges and outgoing edges as interchangeable in the case of directed temporal networks. Therefore, we consider the in- and out- temporal correlation coefficients, denoted by γ_i^{in} and γ_i^{out}, respectively, to focus on the persistence of incoming or outgoing edges. These temporal correlation coefficients for the ith node are defined by

$$\gamma_i^{\text{in}} = \frac{1}{T-1} \sum_{t=1}^{T-1} \frac{\sum_{j=1}^{N} A_{ji}(t) A_{ji}(t+1)}{\sqrt{\left(\sum_{j=1}^{N} A_{ji}(t)\right)\left(\sum_{j=1}^{N} A_{ji}(t+1)\right)}}, \tag{6}$$

$$\gamma_i^{\text{out}} = \frac{1}{T-1} \sum_{t=1}^{T-1} \frac{\sum_{j=1}^{N} A_{ij}(t) A_{ij}(t+1)}{\sqrt{\left(\sum_{j=1}^{N} A_{ij}(t)\right)\left(\sum_{j=1}^{N} A_{ij}(t+1)\right)}}. \tag{7}$$

All temporal correlation coefficients described herein range between 0 and 1.

Statistical methods

Estimating the distribution of overdose journey lengths

The accuracy of overdose journey distances is constrained by the censoring of granular location data (Sect. "EMS data"). To handle this constraint, we apply a method to reconstruct the distribution of transportation event distance (McCabe 2024) to approximate the distributions of overdose journey lengths from FIPS codes. In particular, we carry out the following steps:

1. *Boundary coordinate retrieval*: We obtain the latitude and longitude coordinates of points lying on the boundary of each FIPS code from the TIGER system, which provides shape files for counties.
2. *Range estimation*: For each pair of FIPS codes, we calculate the shortest distance from any point on the boundary of the first to any point on the boundary of the second, according to "as-the-crow-flies" Haversine distance. The resulting range of distances provides a range within which a lower-bound distance between the overdose event and where the person who experienced an overdose lives.
3. *CDF estimation*: We interpret the calculated distance ranges as interval-censored event records and estimate the corresponding survival function $S(d)$ using the Turnbull estimator (Kaplan and Meier 1958; Turnbull 1976). The cumulative distribution function (CDF) is given by $F(d) = 1 - S(d)$.

We apply two hypothesis-testing procedures to compare pairs of collections of censored overdose journey records (i.e., journeys of type A versus those of type B) in terms of their CDFs, denoted by $F_A(d)$ and $F_B(d)$, estimated in the previous step. We select these procedures because they mitigate the challenges associated with censored location data, and they do not rely on the non-guaranteed proportional hazards assumption common in hypothesis tests comparing survival functions. Of course, both procedures assume that the distributions of overdose journey lengths are well-estimated by steps 1–3 above.

In the first method, we employ the so-called Monte Carlo U-test for censored events, a stochastic dominance test for censored transportation event records based on an inverse transform sampling (McCabe 2024). In particular, we repeatedly draw samples from $F_A(d)$ and $F_B(d)$ and conduct Mann–Whitney U-tests for each sample (Mann and Whitney 1947). The p-values from the U-tests are then aggregated using Fisher's combined probability test (Fisher 1932). This approach inherits the assumptions of the U-test and Fisher's method: we assume independence of observations for the sampled journey lengths and independence among the U-tests.

In the second method, we apply a Z-test for the difference in the mean journey length. Specifically, we compute a Z statistic and its corresponding two-tailed p value by $Z = (m_A - m_B)/\sqrt{(\sigma_A^2/n_A) + (\sigma_B^2/n_B)}$ and $p = 2\Phi(-|Z|)$, where m_A, σ_A, and n_A are the mean of $F_A(d)$, the standard deviation of $F_A(d)$, and the number of samples used for estimating $F_A(d)$, and similar for m_B, σ_B, and n_B. Function Φ denotes the CDF of the standard normal distribution. This approach is similar to the test of differences in so-called Restricted Mean Survival Time (RMST) found in clinical trials literature (Royston and Parmar 2011, 2013). Although the true mean and standard deviation of journey lengths can be theoretically obtainable via analytical integration of the true CDFs, they are not known. This test relies on the assumption that m_A, σ_A, m_B, and σ_B are well-estimated via numerical integration of $F_A(d)$ and $F_B(d)$.

Other statistical analyses

We employ several hypothesis tests other than the U- and Z-tests described in Sect. "Estimating the distribution of overdose journey lengths". For group comparisons based on contingency tables, we apply the G-test, which is a log-likelihood ratio-based goodness-of-fit test (McDonald 2014). It is an alternative to the more common chi-squared test, but is often recommended instead on theoretical and practical grounds (Sokal and Rohlf 1987). When assessing differences in means, we invoke Tukey's honestly significant difference (HSD) test. We choose the HSD test instead of alternatives involving analysis of variance with subsequent pairwise comparisons, because HSD automatically corrects for multiple comparisons (Tukey 1949; Kramer 1956; Abdi and Williams 2010). When testing the significance of a trend of a time series, we conduct the Hamed and Rao trend test (Hamed and Rao 1998) over the original Mann-Kendall method (Kendall 1975) because the former test accounts for the effects of autocorrelation. When performing multiple comparisons with tests that do not automatically account for them, we apply the Holm-Bonferroni correction to control family-wise error rate (Holm 1979). This procedure ensures that the false positive rate does not exceed the significance level, while maintaining a lower false negative rate than the Bonferroni adjustment (Abdi 2010).

The activities described in this paper were reviewed by CDC and conducted consistently with applicable federal law and CDC policy.

Results

Basic properties

After applying our exclusion criteria (Sect. "EMS data"), we are left with $N = 481$ counties from 19 states. We show basic structural properties of the overdose journey network

Table 1 Basic network properties of the overdose journey network

Self-loops	Included	Excluded
Number of nodes	482	481
Number of edges	4845	4363
Maximum weighted in-degree	74612	1667
Maximum weighted out-degree	73533	1000
Mean weighted in/out-degree	1034.19	65.25
Maximum unweighted in-degree	106	105
Maximum unweighted out-degree	61	60
Mean unweighted in/out-degree	10.05	9.07
Reciprocity	0.436	0.484

"Included" and "excluded" refer to the networks including and excluding the self-loops, respectively

in Table 1. The overwhelming majority of events (93.7%, 467096 events) occur within the FIPS code of residence of the person who experienced an overdose, represented by self-loops. However, approximately 6.3% (31385 events) occur outside the FIPS code of residence of the person who experienced an overdose. Such events are geographically discordant and are the focus of this work. Of these geographically discordant overdose events, 70% occurred between geographically adjacent counties, and 30% between non-adjacent counties.

Degree analysis

We investigate relationships between the weighted in-degree, weighted out-degree, and the population. Because the network degrees and city populations often obey heavy-tailed distributions (Clauset et al. 2009), we take the logarithm of these three quantities and show the scattergram and R^2 between each pair of the quantities in Fig. 2. The figure indicates that these three quantities are strongly positively correlated with each other. We
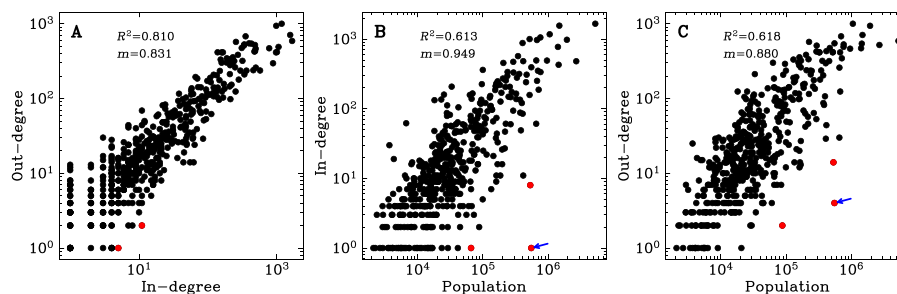

Fig. 2 Relationships between the weighted in-degree, weighted out-degree, and population of the node. **A** Relationships between the weighted in-degree and the weighted out-degree in the overdose journey network excluding self-loops. **B** Relationship between the weighted out-degree and the population. **C** Relationships between the weighted in-degree and the population. In-degree and out-degree values have been incremented by one to ensure visibility in log-transformed space. In all three cases, the weighted degrees exhibit slightly sub-linear relationships as functions of population size. The R^2 values represent correlations between log-transformed values. The m values represent the slopes of the linear regression in the log-transformed space. Outlier points, i.e., counties for which the magnitude of the residuals between observed values and those predicted by the linear regression exceed three standard deviations, are highlighted in red. The blue arrows indicate the county that is an outlier in both panels B and C

also observe slightly sub-linear relationships for the weighted degrees as a function of the population, which suggests a saturation effect of high-population counties as destinations and sources of overdose behavior (Fig. 2B and C). These results are qualitatively the same for unweighted in- and out-degrees, although the correlation is weaker (Fig. 11).

We define outlier points as those whose absolute value of the residual obtained from the linear regression in the log-transformed space exceeds three standard deviations. We show the outlier points in red in Fig. 2. Of particular interest is the one county that is an outlier in both Fig. 2B and C (indicated with a blue arrow), representing disproportionately low geographically discordant overdose activity. This county is a particularly Hispanic and Latino medium metropolitan area that serves as a commuter county for three nearby large metropolitan areas.

To better understand focal points of geographically discordant overdose activity, we consider the top ten counties by the weighted in-degree per capita (top IPC counties) and top ten counties by the weighted out-degree per capita (top OPC counties), representing disproportionately high imports and exports of opioid overdoses when normalized by county population. Even after adjusting for population size, these top counties are exclusively urban counties (Table 2), but they do not simply reflect the largest cities. The top IPC counties are roughly equally represented across large central metro, large fringe metro, and medium metro areas, whereas the top OPC counties are concentrated in large central metro and large fringe metro areas (Table 5). Notably, the top IPC and top OPC counties have populations an order of magnitude larger and significantly higher employment rates than counties that are neither. This may be explained by differences in urbanicity alone: cities are larger and have more jobs than non-cities. The group difference between the top IPC counties and the others in terms of poverty rate is not statistically significant ($p = 0.139$), nor is the difference between the top IPC and top OPC counties in terms of population size ($p = 0.995$). All other group differences are significant ($p < 0.05$). The test results are provided in Table 7.

Table 2 Urbanization, demographic, and socioeconomic profiles of the top ten counties by in-degree per capita (top IPC) and out-degree per capita (top OPC), compared to the remaining counties

	Category	Top IPC	Top OPC	Other
Population	Mean population	1384559	1370947	70262
Urbanicity	Urban	100.0%	100.0%	30.57%
	Rural	0.0%	0.0%	60.43%
Race and ethnicity	White alone	53.88%	55.66%	71.27%
	Black alone	26.83%	24.21%	15.61%
	AI/AN alone	0.352%	0.331%	0.900%
	Asian alone	5.365%	5.579%	2.208%
	NHPI alone	0.056%	0.048%	0.075%
	Hispanic or Latino	21.72%	23.09%	16.54%
Economic	Employed	52.84%	52.68%	48.25%
	Poverty	12.90%	12.30%	13.10%

AI/AN stands for American Indian and Alaska Native. NHPI stands for Native Hawaiian and other Pacific Islander. The top IPC and OPC counties are exclusively urban. Poverty refers to the fraction of the population living below poverty level. The urbanicity values are not population-weighted. Urbanization categories are collapsed into urban and rural per Sect. "Other data". The corresponding results for the uncollapsed urbanization categories are shown in Table 5

Table 3 Urbanization, demographic, and socioeconomic profiles of the top ten and authorities and hubs, compared to the remaining counties

	Category	Authority	Hub	Other
Population	Mean population	1552178	952128	71659
Urbanicity	Urban	100.0%	100.0%	39.96%
	Rural	0.0%	0.0%	60.04%
Race and ethnicity	White alone	55.83%	59.15%	70.98%
	Black alone	21.43%	20.35%	17.28%
	AI/AN alone	0.367%	0.290%	0.878%
	Asian alone	5.086%	3.821%	2.270%
	NHPI alone	0.046%	0.036%	0.0816%
	Hispanic or Latino	32.94%	35.00%	11.96%
Economic	Employed	52.96%	52.60%	48.13%
	Poverty	12.62%	12.13%	13.03%

AI/AN stands for American Indian and Alaska Native. NHPI stands for Native Hawaiian and other Pacific Islander. Like the top IPC and OPC counties, the top hub and authority counties are exclusively urban. Hubs have significantly smaller average populations than authority, top IPC, or top OPC counties. Poverty refers to the fraction of the population living below poverty level. The urbanicity values are not population-weighted. Urbanization categories are collapsed into urban and rural per Sect. "Other data". The corresponding results for the uncollapsed urbanization categories are shown in Table 6

HITS analysis

We similarly characterize in Table 3 the counties with the highest authority and hub scores in comparison to all other counties. Hubs and authorities are over-represented in large fringe metro areas (Table 6). However, despite its name, a large fringe metro county in a large MSA may have a relatively small population because urban-rural classifications depend on MSA populations. In fact, on average, while the top authorities have approximately 12% larger populations than the top IPC and OPC counties, the top hubs have roughly 61% the populations of the top authorities and 69% that of the top IPC and OPC counties (see Table 3). This result is in stark contrast with the observation that the mean population is only approximately 1% different between the top IPC and the top OPC counties (Table 2). Additionally, hub counties have a lower poverty rate than the top authorities or the other counties. All reported group differences are significant with $p < 0.01$. The test results are provided in Table 7.

Lengths of geographically discordant overdose journeys

Figure 3 shows the distribution of journey-to-overdose lengths, denoted by d, among the geographically discordant overdose events. The histogram mass to the right of a particular lower-bound distance d represents the number of events recorded of length at least d (Fig. 3A). Similarly, the histogram mass to the left of a particular upper-bound distance d represents the number of events recorded of length at most d (Fig. 3B). From these lower-bound and upper-bound distances, we estimate the distribution of journey distances as described in Sect. "Estimating the distribution of overdose journey lengths". Figure 3C displays the resultant estimated complementary CDF (i.e., survival function) of d.

From our estimation, the median and mean distance of geographically discordant overdose journeys is 47.54 km and 105.4 km, respectively (Fig. 3D). Unsurprisingly, events are more common close to the home of a person who experienced an overdose.
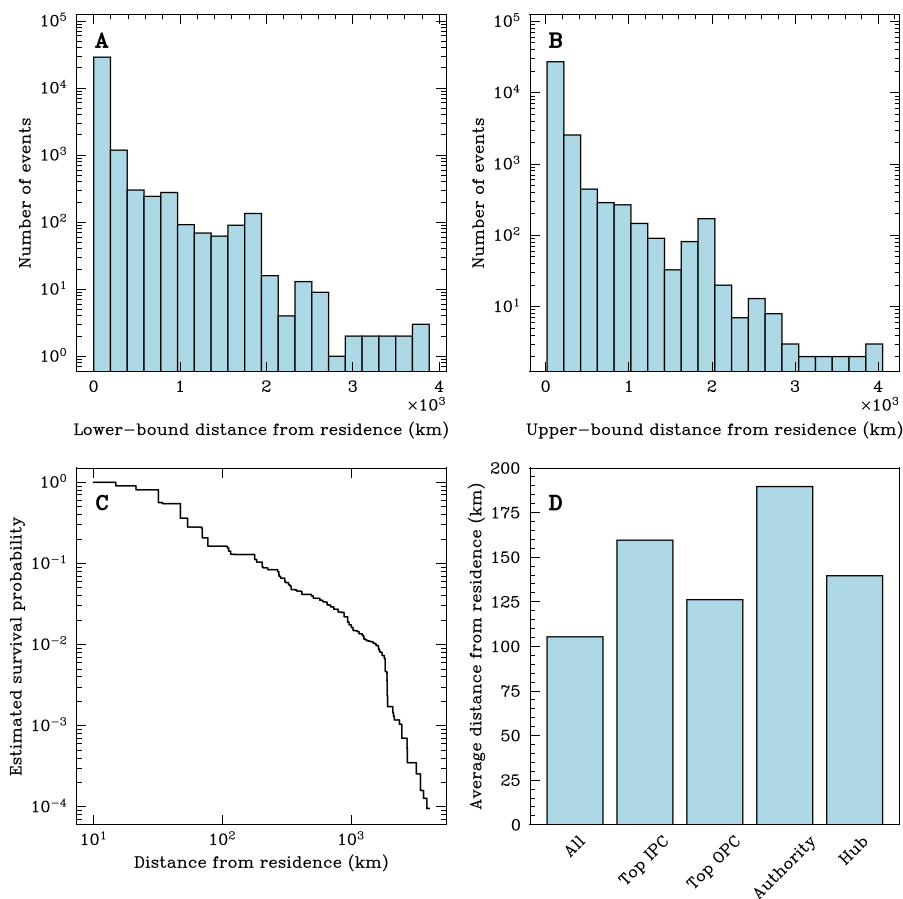
Fig. 3 Distribution of distances of geographically discordant overdose journeys. **A** Empirical distribution of lower-bound distances among the journeys. **B** Empirical distribution of upper-bound distances. **C** Estimated survival function of the journey distance. **D** Average distance of geographically discordant overdose journeys. "All" refers to all journeys. "Top IPC," "Top OPC," "Authority," and "Hub" refer to journeys to the top IPC, OPC, authority, and hub counties, respectively.

However, approximately 10% of the journeys exceed 204.38 km, and 5% exceed 342.56 km. Figure 3C indicates a heavy-tailed nature of the distribution. Indeed, the coefficient of variation (CV) of d, i.e., the standard deviation of d divided by the mean of d, is substantially larger than 1 (CV = 2.330), indicating that the distribution of d has a heavier tail than the exponential distribution.

In Fig. 3D, we interpret the journey-to-overdose distance as an import or export radius. In particular, we investigate the average journey-to-overdose distance *to* importers for the top IPC and authority counties and *from* exporters for the top OPC and hub counties. As reference, we also show the journey distance averaged over all the journeys (see the "All" bar in Fig. 3D). The geographically discordant overdose journey from the residence to the top IPC counties and from the top OPC counties to their destinations are both longer, on average, than the mean journey. Furthermore, the journey distance for the top IPC counties is larger than that for the top OPC counties on average. As expected, the average journey distance to the top authority counties and from the top hub counties show qualitatively the same behavior as that to the top IPC counties and that from the

top OPC counties, respectively. In other words, the average distance to the top authority counties is larger than that from the top hub counties, and the latter is larger than the average over all geographically discordant journeys. However, the effects of authorities and hubs are not a straightforward consequence of the general fact that authorities and hubs tend to be counties with large in-degrees and large out-degrees, respectively. In fact, Fig. 3D suggests that the average journey distance is larger for the top authority counties than the top IPC counties and larger for the top hub counties than the top OPC counties. See the "Monte Carlo U-Test" and "Z-Test" columns of Table 8 for statistical results.

Temporal aspects

We decompose the overdose journey network into a time series of overdose journey networks by constructing the network for each six-month time window. We show the time series of the share of the self-loops and the average journey distance in Fig. 4A and B, respectively, in which each data point represents a six-month time window. The portion of the overdose events occurring in the person's home county increased throughout 2018–2023 (Fig. 4A). The average and median journey distance for geographically discordant overdose events did not systematically increase or decrease over the same five years, including the wake of the COVID-19 pandemic, which is shown by the dashed line (Fig. 4B).

Whether edges of the journey network are consistently present from one time period to another is relevant for public health applications. Such persistence reflects enduring overdose-related transit patterns that may warrant policy intervention. To quantify the persistence of edges, we obtain the undirected temporal correlation coefficient $\gamma = 0.303$. Further, focal importers and exporters (i.e., the top IPC, OPC, authority, and hub counties) exhibit a significantly greater probability of (undirected) incident edge persistence than the average over all counties ($p < 0.05$), with γ nearly double the network's average (Fig. 5A). Approximately the same results hold true in the directed setting, as
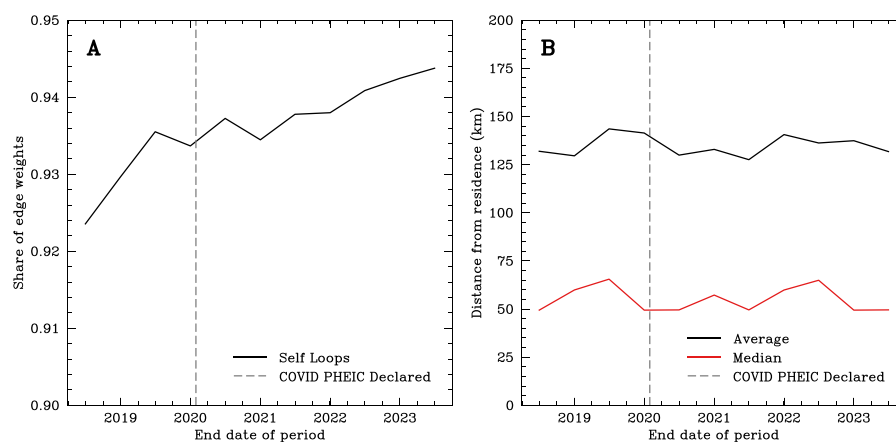

Fig. 4 Time courses of the fraction of self-loops and the overdose journey distance. **A** Fraction of edge weights owing to self-loops, indicating the portion of overdose events occurring in the home county of the person who experienced an overdose. **B** Average and median journey distance for geographically discordant events. The dashed lines indicate the date at which the World Health Organization declared the beginning of the COVID-19 Public Health Emergency of International Concern (PHEIC) (Fadel and Aizenman 2023)
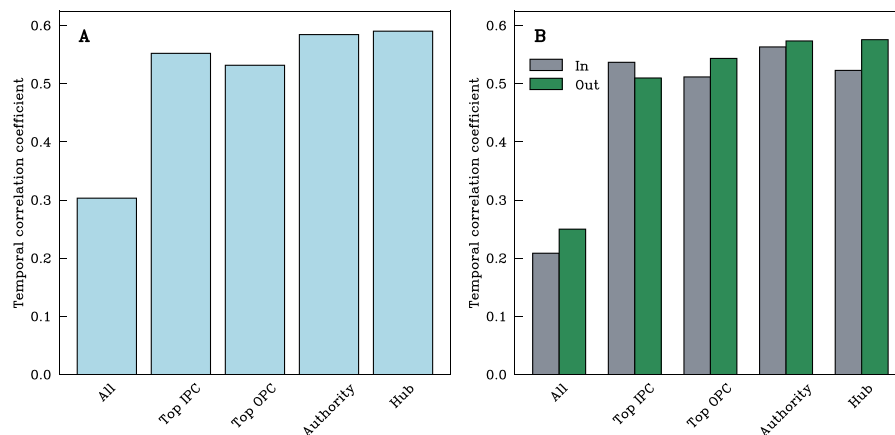
Fig. 5 Persistence of edges in the temporal overdose journey network. **A** Average undirected temporal correlation coefficients for all counties, and the top IPC, OPC, authority, and hub counties. **B** Average directed (i.e., in- and out-) temporal correlation coefficients for all counties, and the top IPC, OPC, authority, and hub counties. In both the undirected and directed settings, focal importers and exporters have greater-than-average temporal correlation coefficients

well: focal importers and exporters also have significantly greater in- and out- temporal correlation coefficients than the network's average ($p < 0.05$, Fig. 5B).

Discussion

We analyzed a spatial network of opioid-involved overdose journeys from 19 states across the U.S. constructed from EMS records spanning 2018–2023. Our work underscores that the opioid overdose epidemic does not only exist where overdoses occur. Patterns of import and export of overdose behavior across county borders emerge, as more than 6% of opioid-involved overdose events occurred outside the residential FIPS code of the person who experienced an overdose. We focused on these geographically discordant events, of which roughly 10% occurred over 204 km from the home of the person who experienced an overdose. It is itself noteworthy, however, that nearly 94% of opioid-involved overdoses occurred within the county of residence of the person who experienced the overdose, suggesting that the majority of persons overdosed in their home communities. Thus, assessment of either the location of the overdose event or the documented patient residence can be used to understand focal locations for overdoses, such that harm reduction services (e.g., naloxone and fentanyl test strip distribution) and services for linking to care and treatment can be deployed more effectively.

Public health authorities may wish to identify and intervene at focal points of import/export behavior, but it is not necessarily clear how to define them. In this work, we considered two such approaches: measures calculable from normalized travel counts involving the county alone (i.e., IPC and OPC) and network-based measures (i.e., authorities and hubs). Focal counties according to these measures tended to be urban, were higher in Black, Asian, and Hispanic or Latino populations, were lower in white, American Indian and Alaska Native, and Native Hawaiian and other Pacific Islander populations, and had a larger employment rate, population, journey distance, and edge persistence than the average over all the edges in the network.

We found that some aspects of overdose journeys differed between the types of focal points. For instance, the top IPC, OPC, and authority counties have population sizes of the same order of magnitude on average, but the top hubs are much smaller in population, although they are much larger than the average over all counties. Additionally, the overdose journeys to the top IPC and authority counties were longer than those from the top OPC and hub counties on average. This result may be partly explained by size and resource advantage: the average population of authorities is more than twice that of hubs, and larger counties may provide more resources for opioid users (Chatterjee et al. 2022).

We contend that indirect paths in the overdose journey network do not have functional meanings for the following reason: If there is an indirect path from the ith to the ℓth nodes, then $A_{ij} = 1$ and $A_{j\ell} = 1$, which implies that there is an overdose journey from the ith to the jth nodes, made by individual u_1, and another journey from the jth to the ℓth nodes, made by individual u_2. In this situation, it is unlikely that u_1 influences u_2 to trigger u_2's overdose behavior outside u_2's residence. The same reasoning holds true even if edges are weighted or we consider the effects of mass media or social media. The difficulty of interpretation of indirect paths may limit the utility of network analysis as an approach, rendering only the direct path effects such as the in- and out-degrees relevant to overdose behavior. However, we found that the HITS algorithm, which exploits effects of the indirect paths (e.g., hub scores of nodes are large when they send edges to authorities, which are nodes that tend to receive edges from hubs), reveals features of overdose journeys that were beyond the prediction by the top IPC or OPC counties. Specifically, the top authority and hub counties had larger journey distances than the top IPC and OPC counties, respectively. In addition, the top authorities, top hubs, and top OPC counties tend to be concentrated in large fringe metropolitan areas, whereas top IPC counties are more dispersed across large central metropolitan, large fringe metropolitan, and medium metropolitan areas. These results suggest that the authorities and hubs, which tend to be interconnected with each other, may form a scaffold of the overdose journey network and have particular properties compared to top IPC and OPC counties. Further investigating this issue in combination with other data sources, demographic information, and geographic information, with potentially improved coverage and accuracy of the EMS records, warrants future work.

We showed in Sect. "Temporal aspects" that the share of geographically discordant events decreased between 2018 and 2023. This result is consistent with recent evidence from Rhode Island suggesting that drug overdose deaths occurring in residences of the people who experienced overdoses increased disproportionately from 2019 to 2020 (Macmadu et al. 2021). Among geographically discordant events, however, we did not observe a decrease in overdose journey distance after the beginning of the COVID-19 pandemic. Future work examining the individual-level profiles of this type of overdose journey would enhance this line of inquiry.

Our estimate of the fraction of geographically discordant overdose events is much lower than the 25% reported in a recent study (Forati et al. 2023). There are at least two potential reasons causing this difference. First, their work examined overdose deaths, whereas we focused on nonfatal incidents. Second, we use differently sized geographic units: counties in the present study versus census tracts in their study. Therefore, our criteria for geographical discordance is technically stricter than theirs, excluding many events

that could be considered discordant by the definition used in their work. In addition to these differences, our larger scale of analysis enabled us to identify inter-county overdose journeys and analyze the distribution of overdose journey distances. Another advancement of the present study relative to theirs is that we compared between authority counties and top IPC counties and between hub counties and top OPC counties. With the latter analysis, we provided evidence supporting that the HITS algorithm provides unique information about overdose journeys that simpler pairwise analysis does not.

Our work has at least four potential limitations. First, we are limited by data availability because we have few or no records for many states in the U.S. This may introduce bias in our results and limit generalizability, since the availability of EMS data may be influenced by latent confounders. That is, our end-to-end selection process may not have resulted in a uniformly random subset of all nonfatal opioid-involved overdose events. Furthermore, U.S. demographics have significant spatial variability, and many aspects of the opioid epidemic have racial covariates (Santoro and Santoro 2018; Gondré-Lewis et al. 2023), which probably contribute to heterogeneity in overdose journey statistics across states.

Second, related to the first limitation, we restricted our analysis to the counties with at least 75% UEC for the entire five-year period. Doing so is standard for the present data set (Casillas et al. 2022) but excludes many counties (Sect. "EMS data"). Future data collection efforts may mitigate this limitation, as the number of reporting counties increases. Third, we focused on non-fatal opioid-involved overdose events, which may mean that our characterizations of journey lengths is not fully representative of high-mortality counties. Fourth, our EMS event records are geographically censored at the county-equivalent level. Therefore, we make no claims about spatial dynamics for within-county overdose journeys. Additionally, we rely on survival analysis-based procedures for estimating the distributions of overdose journey lengths. Since these approaches are limited by the quality of survival function estimation, future work may aim to narrow these data gaps to draw more granular insights regarding the national character of overdose journeys. Future work can also focus on different types of drugs, such as stimulants, to compare the spatial dynamics of different non-fatal overdoses across the country. In the U.S., the overdose death rate involving psychostimulants with abuse potential (e.g., methamphetamine) has historically been higher in rural counties than urban ones (Spencer et al. 2022a). We are not aware of any work examining network patterns of stimulant-involving overdose journeys. Further, more comprehensive analysis of socioeconomic variables may provide a richer characterization of overdose journeys. Of particular interest are proxies of healthcare access, such as primary care physicians per unit population (County Health Rankings and Roadmaps 2024) or response to related questions in the CDC's Behavioral Risk Factor Surveillance System (Silva 2014; Buchmueller and Levy 2020).

We highlight the value of leveraging large-scale EMS data for understanding the spatial dynamics of the opioid crisis. While spatially aggregated EMS records allow researchers to conduct analyses while preserving patient privacy, there are important limitations arising from data availability and completeness. These may be partially ameliorated as coverage and reporting rates steadily rise, but this may take a long time. Future work should consider if integration of external and partially redundant data sources can support analyses such as the present study with lower minimum UEC levels. A second potential avenue for future research is to leverage agent-based simulation, which has already been used to study spatio-temporal dynamics of opioid use disorder (Grefenstette et al. 2013), to better understand

the efficacy of targeting authorities and hubs for public health interventions. Of particular interest is the relationship between the number and strategic placement of harm-reduction and emergency room facilities and overdose journey length. Ambulance journey distance has been shown to be correlated with patient mortality (Nicholl et al. 2007), so a function of overdose journey length may be a reasonable proxy for the likelihood of overdose survival in such simulations. Third, further analysis contrasting self-loops and discordant overdose journeys may be fruitful. Such an analysis can involve a review of the type of locations where these events occur (e.g., private residences, public areas such as streets, schools, etc.) or patient demographic characteristics, which may provide more insight into the differences among those who overdosed in their home communities and those who overdosed elsewhere. Then, more tailored public health interventions may be deployed. A fourth future research thrust is to better understand the especially long overdose journeys highlighted in this study. In "Sect. 'Lengths of geographically discordant overdose journeys'", we estimate that 5% of geographically discordant incidents occurred over 426 km from the home of the person who experienced an overdose. We emphasize, however, that people who experienced overdoses did not necessarily travel such distances on the days of their incidents. For instance, not all individuals (e.g., those experiencing homelessness) functionally reside in their official residence of record for the entire year. Additionally, EMS place-of-residence information is sometimes collected from historical patient records, which may be out-of-date or inaccurate due to clerical errors. Further research is required to better understand the etiology of these particularly long overdose journeys.

Appendix A
Acronyms used in this work
See Table 4.

Table 4 A selection of acronyms used in this article

Acronym	Full form	Description
ACS	American Community Survey	Annual demographics survey of approximately 3.5 million U.S. addresses managed by the U.S. Census, providing details on education, employment, housing, and more.
CSTE	Council of State and Territorial Epidemiologists	U.S. non-profit public health organization.
EMS	Emergency Medical Services	A healthcare system offering first-respondent care to medical emergencies.
FIPS	Federal Information Processing Standards	Numerical codes assigned by the National Institute of Standards and Technology (NIST) to uniquely represent U.S. states and counties (including county equivalents).
NCHS	National Center for Health Statistics	Agency of the U.S. Centers for Disease Control and Prevention (CDC) providing public health statistical information.
UEC	Underlying Event Coverage	Proprietary metric by biospatial estimating the portion of total EMS events in a given area captured in the biospatial platform for a given time period.
URCS	Urban-Rural Classification Scheme for Counties	Classification system provided by the U.S. National Center for Health Statistics (NCHS) assigning each U.S. county to one of six urban categories.
TIGER	Topologically Integrated Geographic Encoding and Referencing	System maintained by the U.S. Census providing digital cartographic information of U.S. geographic areas.

Distribution of UEC

See Fig. 6.

Sensitivity to the UEC threshold

In Sect. "EMS data", we exclude counties with the minimum UEC below 75%, following earlier work with this dataset (Casillas et al. 2022). We note that, if G_β is the overdose journey network arising from our dataset using a minimum UEC threshold β, then, for $\beta_1 > \beta_2$, G_{β_1} is a subgraph of G_{β_2}. Therefore, we carry out the following three sensitivity analyses to confirm that our main results are not too strongly sensitive to our choice of the β value (i.e., 75%).

First, we examine sensitivity of the relationships between the weighted in-degree, weighted out-degree, and population of counties (examined in Fig. 2) to the variation
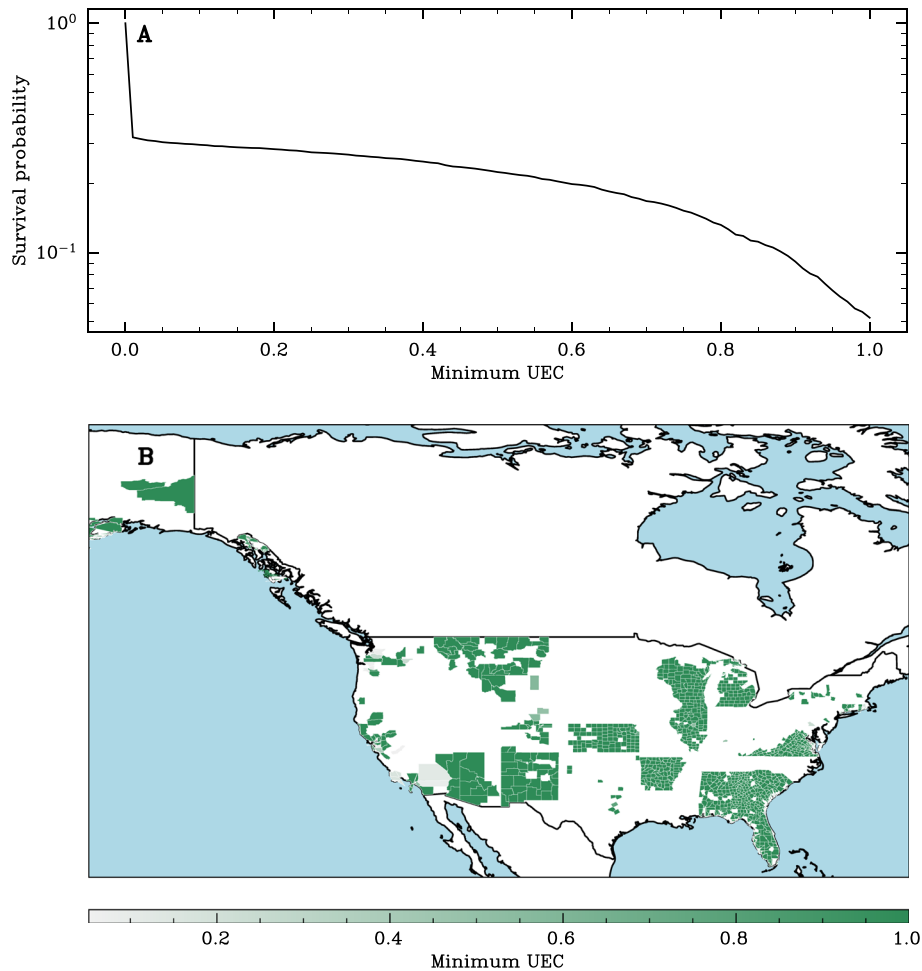
Fig. 6 Visualization of each county's minimum UEC. For each county, we have computed the lowest UEC value between January 2018 and March 2023. This is after sub-setting our data to nonfatal opioid occurrences but prior to filtering out counties with the threshold of 75% minimum UEC. **A** Empirical survival function (i.e., complementary cumulative distribution) of the minimum UEC. **B** Heatmap of the minimum UEC across U.S. counties. White indicates the absence of data (i.e., no coverage in any time period). The lightest grey-green indicates a minimum UEC of zero (i.e., no coverage in at least one but not all time periods)

in the β value. Figure 7A and B shows that the slope and correlation coefficient, respectively, of the linear regression vary little, except those involving the population when $\beta = 0.85$ (red and blue lines in the figure). Second, our distance-to-overdose results (examined in Fig. 3D) are qualitatively similar between $\beta = 0.55$ and $\beta = 0.75$ (see Fig. 8A–C), whereas the prominence of the top authority counties is lost at $\beta = 0.85$ (Fig. 8D). Third, we analyze the edge persistence (examined in Fig. 5) for different values of β to find that the results are qualitatively comparable across the β values (see Fig. 9). Specifically, the top importers and exporters show notably greater temporal correlation coefficients than the network's average, in both undirected and directed settings.

With Figs. 7, 8, and 9, we conclude that the results are reasonably robust against variation in the β value, at least between $\beta = 0.55$ and $\beta = 0.75$.
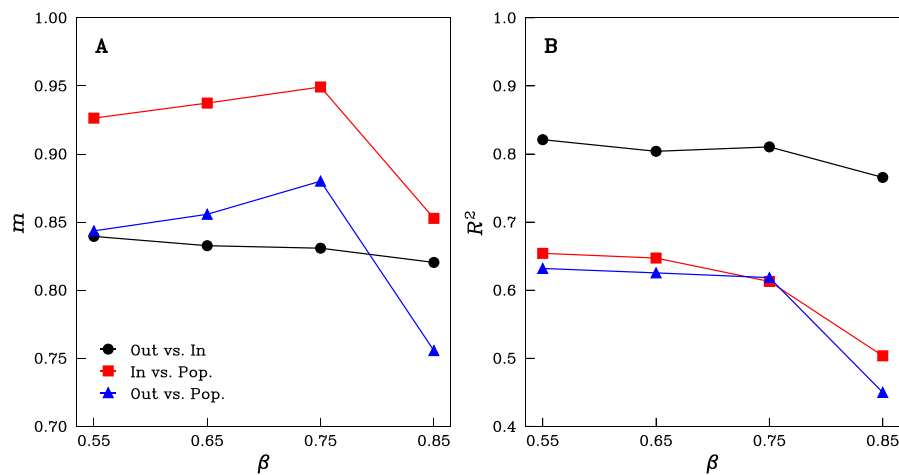
Fig. 7 Dependence of the pairwise correlation between the weighted in-degree, weighted out-degree, and population of nodes on the UEC threshold. **A** Linear regression slopes (m) between the weighted out-degree and the weighted in-degree (out vs. in), between the weighted in-degree and the population (in vs. pop.), and between the weighted out-degree and the population (out vs. pop.) in the log-transformed space, as in Fig. 2. **B** Correlation coefficients, R^2, for the same linear regression. Slopes and correlation coefficients involving the population are dampened with $\beta = 0.85$. Otherwise, m and R^2 values are generally consistent across values of β
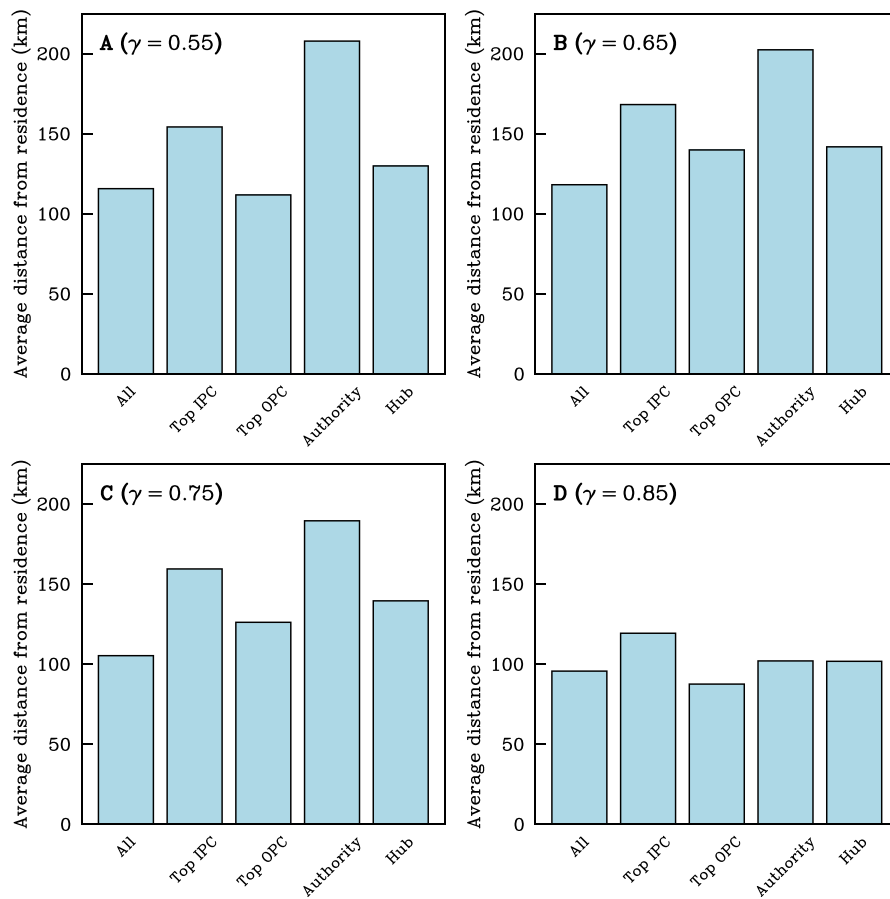
Fig. 8 Dependence of the county's average overdose journey distance on the UEC threshold. **A** $\beta = 0.55$. **B** $\beta = 0.65$. **C** $\beta = 0.75$. **D** $\beta = 0.85$. Panel C replicates Fig. 3D in the main text. The results are similar among $\beta = 0.55$, 0.65, and 0.75, whereas the results for the top authority counties are dampened for $\beta = 0.85$
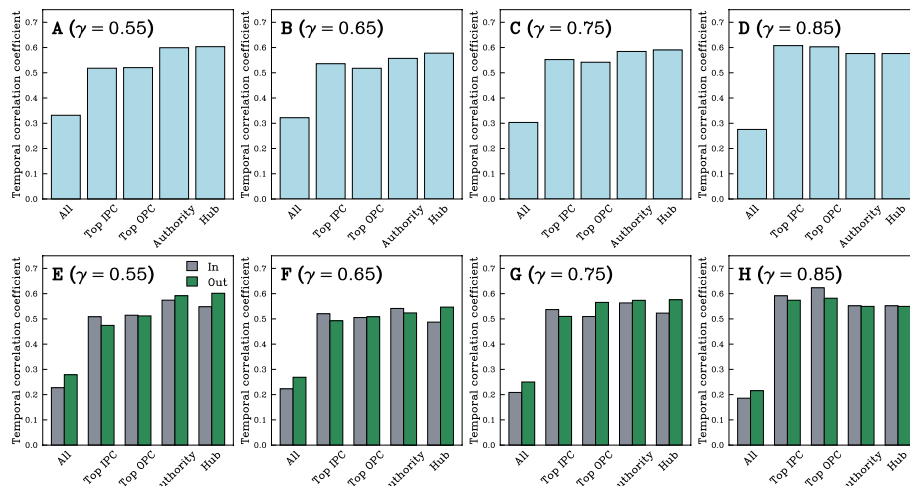

Fig. 9 Dependence on the county's temporal correlation coefficient on the UEC threshold. **A** Undirected, $\beta = 0.55$. **B** Undirected, $\beta = 0.65$. **C** Undirected, $\beta = 0.75$. **D** Undirected, $\beta = 0.85$. **E** Directed, $\beta = 0.55$. **F** Directed, $\beta = 0.65$. **G** Directed, $\beta = 0.75$. **H** Directed, $\beta = 0.85$. Panels C and G replicate Figs. 5A and B, respectively, in the main text. We find that the results are qualitatively consistent across these values of β

Top *k* selection

Throughout this work, we consider top *k* counties across four metrics. To set the *k* value, we first sort the weighted in-degree per capita, weighted out-degree per capita, hub score, and authority score, of all the counties. Then, for each of these metrics, we calculate the elbow point (i.e., the metric value yielding the maximum curvature) using the offline Kneedle algorithm. We set the algorithm's sensitivity parameter *S* to 0, which is recommended in perfect information settings (Satopaa et al. 2011).

This process reveals elbow values of 11, 10, 3, and 4 for weighted in-degree per capita, weighted out-degree per capita, authority scores, and hub scores, respectively (Fig. 10). In the interest of readability, interpretability, and consistency, we use *k* = 10 for all the four metrics. This *k* value is a round number close to or equal to the elbow values for the IPC and OPC, respectively. It is important to use the same *k* value across the four measures because we compare observations from the top *k* counties (e.g., average distance of geographically discordant overdose journey over the top *k* counties) across the four measures.
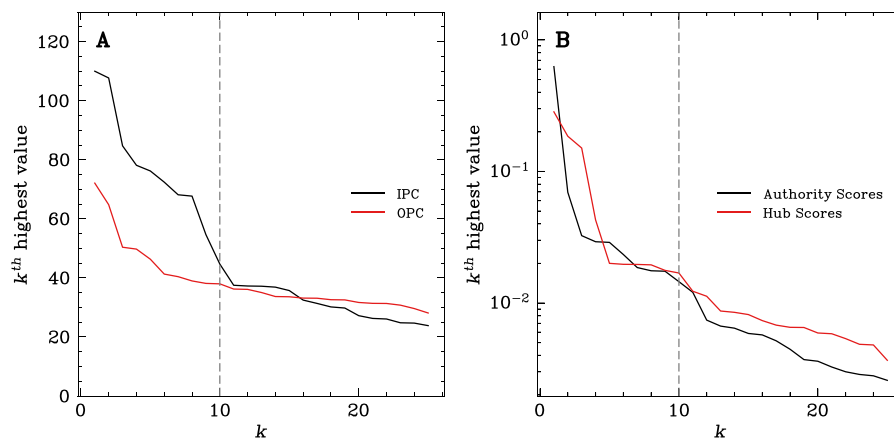

Fig. 10 Sorted IPC, OPC, authority, and hub values. **A** Sorted IPC and OPC values. **B** Sorted authority and hub scores. We selected *k* = 10, indicated by the dashed lines, because it is a round number near the IPC and OPC elbow values
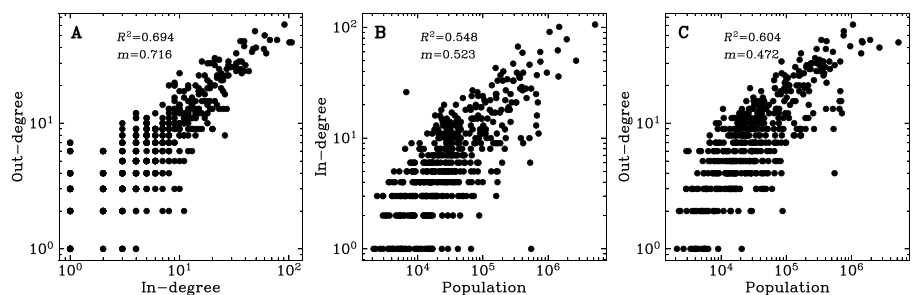
Fig. 11 Relationships between the unweighted in-degree, unweighted out-degree, and population of the node. **A** Relationships between the unweighted in-degree and the unweighted out-degree in the overdose journey network excluding self-loops. **B** Relationship between the unweighted out-degree and the population. **C** Relationships between the unweighted in-degree and the population. The unweighted in- and out- degrees sub-linearly depend on the population size. The slopes of the linear regression in the log-transformed space are smaller than those for the weighted degree shown in Fig. 2. In-degree and out-degree values have been incremented by one to ensure visibility in log-transformed space. The R^2 values represent correlations between log-transformed values to limit distortion from outliers. The m values represent the slopes of the linear regression in the log-transformed space

Unweighted degree analysis
See Fig. 11.

County profiles with uncollapsed urbanization categories
See Tables 5 and 6.

Statistical results
See Tables 7 and 8.

Table 5 Urbanization profiles of the top ten counties by in-degree per capita (top IPCs) and out-degree per capita (top OPCs), compared to the remaining counties

	Category	Top IPC (%)	Top OPC (%)	Other (%)
Urbanicity	Large central metro	40.0	30.0	1.290
	Large fringe metro	30.0	60.0	13.76
	Medium metro	30.0	10.0	12.26
	Small metro	0.0	0.0	12.26
	Micropolitan	0.0	0.0	17.20
	Noncore	0.0	0.0	43.23

Values are not population-weighted

Table 6 Urbanization profiles of the top ten authorities and hubs, compared to the remaining counties

	Category	Authority (%)	Hub (%)	Other (%)
Urbanicity	Large central metro	30.0	20.0	1.496
	Large fringe metro	70.0	60.0	13.68
	Medium metro	0.0	10.0	12.82
	Small metro	0.0	10.0	11.97
	Micropolitan	0.0	0.0	17.09
	Noncore	0.0	0.0	42.95

Values are not population-weighted

Table 7 Statistical results for pairwise comparison between any two of the top IPC, top OPC, and the other counties and between any two of the top authority, top hub, and the other counties

	Population	Race and ethnicity	Employed	Poverty
Top IPC versus top OPC		***	*	***
Top IPC versus other	***	***	***	
Top OPC versus other	***	***	***	***
Authority versus hub	***	***	***	***
Authority versus other	***	***	***	**
Hub versus other	***	***	***	***

In terms of the socioeconomic variables evaluated, all pairwise comparisons from our HITS analysis and all but one pairwise comparisons from our IPC/OPC degree analysis indicate significant differences at the $\alpha = 0.05$ significance level. We ran the Tukey's HSD test, which corrects for multiple comparisons (Tukey 1949; Kramer 1956), for "Population," which refers to the total population size. We used the contingency table-based G-test of independence (McDonald 2014) for "race and ethnicity," "employed," and "poverty." *: $p < 0.05$, **: $p < 0.01$, and ***: $p < 0.001$. All the results obtained with the G-test are Holm–Bonferroni-corrected for $3 \binom{3}{2} = 9$ comparisons (Holm 1979)

Table 8 Statistical results for pairwise comparisons of the journey distances and average temporal correlation coefficients

	Journey distance		Temporal correlation		
	Monte Carlo U-test	Z-test	HSD test (undirected)	HSD test (in)	HSD test (out)
All versus top IPC	***	***	**	***	**
All versus top OPC	***	***	*	***	**
All versus authority	***	***	**	***	***
All versus hub	***	***	**	***	***
Top IPC versus top OPC	***	***			
Top IPC versus authority		***			
Top IPC versus hub		***			
Top OPC versus authority	***	***			
Top OPC versus hub	***	**			
Authority versus hub		***			

All pairwise comparisons indicate significant differences in the mean journey distance at the $\alpha = 0.01$ significance level. The "Monte Carlo U-test" and "Z-test" columns reflect the results for journey distances, for which we ran the Monte Carlo U-test and Z-test described in Sect. "Estimating the distribution of overdose journey lengths". The "HSD Test (undirected)," "HSD test (in)," and "HSD test (out)" columns reflect results for undirected temporal correlation coefficients, in- temporal correlation coefficients, and out- temporal correlation coefficients, respectively, for which we ran Tukey's HSD test (Tukey 1949; Kramer 1956). *: $p < 0.05$, **: $p < 0.01$, and ***: $p < 0.001$. All the results are Holm-Bonferroni-corrected for $\binom{5}{2} = 10$ comparisons (Holm 1979), with the exception of HSD tests, which already correct for multiple comparisons

References

Abdi H (2010) Holm's sequential Bonferroni procedure. Encycl Res Des 1(8):1–8

Abdi H, Williams LJ (2010) Tukey's honestly significant difference (HSD) test. Encycl Res Des 3(1):1–5

Biospatial (2023) EMS Data-Driven Insight | Hosptial Market Intelligence | biospatial. https://www.biospatial.io/

Buchmueller TC, Levy HG (2020) The ACA's impact on racial and ethnic disparities in health insurance coverage and access to care: an examination of how the insurance coverage expansions of the Affordable Care Act have affected disparities related to race and ethnicity. Health Aff 39(3):395–402

Bureau UC (2021) American Community Survey 2017-2021 5-year Data Release. American Community Survey 5-year estimates, https://www.census.gov/newsroom/press-kits/2022/acs-5-year.html

Büttner K, Salau J, Krieter J (2016) Temporal correlation coefficient for directed networks. Springerplus 5(1):1–17

Casillas SM, Pickens CM, Stokes EK et al (2022) Patient-level and county-level trends in nonfatal opioid-involved overdose emergency medical services encounters-491 counties, United States, January 2018–March 2022. Morbidity and mortality weekly report. Vol 71(34), p 1073

Chatterjee A, Yan S, Xuan Z et al (2022) Broadening access to naloxone: community predictors of standing order naloxone distribution in Massachusetts. Drug Alcohol Depend 230:109190

Chen P, Lu Y (2021) Journey-to-crime and offender's geographic background: a comparison between migrant and native offenders in beijing. SN Soc Sci 1(1):36

Clauset A, Eagle N (2007) Persistence and periodicity in a dynamic proximity network. Proceedings of the DIMACS workshop on computational methods for dynamic interaction networks

Clauset A, Shalizi CR, Newman MEJ (2009) Power-law distributions in empirical data. SIAM Rev 51(4):661–703

Council of State and Territorial Epidemiologists (2022) Emergency Medical Services Nonfatal Opioid Overdose Standard Guidance. Standard guidance, Council of State and Territorial Epidemiologists, accessed: September 24, 2023

County Health Rankings & Roadmaps (2024) Primary care physicians. https://www.countyhealthrankings.org/health-data/health-factors/clinical-care/access-to-care/primary-care-physicians?year=2024

Dart RC, Surratt HL, Cicero TJ et al (2015) Trends in opioid analgesic abuse and mortality in the United States. N Engl J Med 372(3):241–248

Donnelly EA, Wagner J, Hughes C et al (2021) Opioids, race, context, and journeys to crime: analyzing black-white differences in travel associated with opioid possession offenses. Crim Justice Behav 48(12):1714–1731

Fadel L, Aizenman N (2023) Who says covid-19 is no longer a global health emergency. https://www.npr.org/2023/05/05/1174275727/who-says-covid-19-is-no-longer-a-global-health-emergency

Fisher RA (1932) Statistical methods for research workers. Oliver and Boyd, Edinburgh

Forati A, Ghose R, Mohebbi F et al (2023) The journey to overdose: using spatial social network analysis as a novel framework to study geographic discordance in overdose deaths. Drug Alcohol Depend 245:109827

Garlaschelli D, Loffredo MI (2004) Patterns of link reciprocity in directed networks. Phys Rev Lett 93(26):268701

Gondré-Lewis MC, Abijo T, Gondré-Lewis TA (2023) The opioid epidemic: a crisis disproportionately impacting Black Americans and urban communities. J Racial Ethn Health Disparities 10(4):2039–2053

Grefenstette JJ, Brown ST, Rosenfeld R et al (2013) FRED (a framework for reconstructing epidemic dynamics): an open-source software system for modeling infectious diseases and control strategies using census-based populations. BMC Public Health 13:1–14

Hamed KH, Rao AR (1998) A modified Mann-Kendall trend test for autocorrelated data. J Hydrol 204(1–4):182–196

Holm S (1979) A simple sequentially rejective multiple test procedure. Scand J Stat 6(2):65–70

Ingram DD, Franco SJ (2014) 2013 NCHS urban-rural classification scheme for counties. Vital Health Stat 166:1–73

Jalal H, Buchanich JM, Roberts MS et al (2018) Changing dynamics of the drug overdose epidemic in the United States from 1979 through 2016. Science 361(6408):eaau1184

Johnson LT, Taylor RB, Ratcliffe JH (2013) Need drugs, will travel?: the distances to crime of illegal drug buyers. J Crim Just 41(3):178–187

Kaplan EL, Meier P (1958) Nonparametric estimation from incomplete observations. J Am Stat Assoc 53(282):457–481

Kendall MG (1975) Rank correlation methods. Charles Griffin, London, UK

Kleinberg JM (1999) Authoritative sources in a hyperlinked environment. J ACM 46(5):604–632

Kramer CY (1956) Extension of multiple range tests to group means with unequal numbers of replications. Biometrics 12(3):307–310

Lee B, Zhao W, Yang KC et al (2021) Systematic evaluation of state policy interventions targeting the us opioid epidemic, 2007–2018. JAMA Netw Open 4(2):e2036687–e2036687

Luke DA, Harris JK (2007) Network analysis in public health: history, methods, and applications. Annu Rev Public Health 28:69–93

Luke DA, Stamatakis KA (2012) Systems science methods in public health: dynamics, networks, and agents. Annu Rev Public Health 33:357–376

Macmadu A, Batthala S, Gabel AMC et al (2021) Comparison of characteristics of deaths from drug overdose before vs during the COVID-19 pandemic in Rhode Island. JAMA Netw Open 4(9):e2125538–e2125538

Mann HB, Whitney DR (1947) On a test of whether one of two random variables is stochastically larger than the other. Ann Math Stat 18:50–60

Masuda N, Lambiotte R (2020) A guide to temporal networks, 2nd edn. World Scientific, Singapore

McCabe LH (2024) Nonparametric estimation and comparison of distance distributions from censored data. In: 2024 58th annual conference on information sciences and systems (CISS), IEEE, pp 1–6

McDonald JH (2014) G-test of goodness-of-fit, 3rd edn. Sparky House Publishing, Baltimore, MD, pp 53–58

Newman MEJ (2018) Networks, 2nd edn. Oxford University Press, Oxford, UK

Newman MEJ, Forrest S, Balthrop J (2002) Email networks and the spread of computer viruses. Phys Rev E 66(3):035101

Nicholl J, West J, Goodacre S et al (2007) The relationship between distance to hospital and patient mortality in emergencies: an observational study. Emerg Med J 24(9):665–668

Nicosia V, Tang J, Mascolo C et al (2013) Graph metrics for temporal networks. Springer, Berlin, DE, pp 15–40

Oser CB, Harp KLH (2015) Treatment outcomes for prescription drug misusers: the negative effect of geographic discordance. J Subst Abuse Treat 48(1):77–84

Perry BL, Yang KC, Kaminski P et al (2019) Co-prescription network reveals social dynamics of opioid doctor shopping. PLoS ONE 14(10):e0223849

Phillips PD (1980) Crime: a spatial perspective. In: Georges-Abeyie DE (ed) Characteristics and typology of the journey to crime. Columbia University Press, New York, pp 167–180

Rengert GF (2002) Crime, policing and place: essays in environmental criminology. In: Evans D, Fyfe N, Herbert D (eds) The journey to crime: conceptual foundations and policy implications. Routledge, London, pp 109–117

Royston P, Parmar MK (2011) The use of restricted mean survival time to estimate the treatment effect in randomized clinical trials when the proportional hazards assumption is in doubt. Stat Med 30(19):2409–2421

Royston P, Parmar MK (2013) Restricted mean survival time: an alternative to the hazard ratio for the design and analysis of randomized trials with a time-to-event outcome. BMC Med Res Methodol 13:152

Rudolph AE, Young AM, Havens JR (2019) Using network and spatial data to better target overdose prevention strategies in rural Appalachia. J Urban Health 96(1):27–37

Santoro TN, Santoro JD (2018) Racial bias in the US opioid epidemic: a review of the history of systemic bias and implications for care. Cureus 10(12):e3733

Satopaa V, Albrecht J, Irwin D, et al. (2011) Finding a "kneedle" in a Haystack: detecting knee points in system behavior. In: 31st international conference on distributed computing systems workshop, IEEE, pp 166–171

Service NW (2023) U.S. counties. https://www.weather.gov/gis/Counties, shape files derived from TIGER 2000. Date uploaded: 30 June 2023

Silva NM (2014) The behavioral risk factor surveillance system. Int J Aging Hum Dev 79(4):336–338

Sokal RR, Rohlf FJ (1987) Introduction to biostatistics. Dover, San Francisco, CA

Spencer MR, Garnett MF, Miniño AM (2022a) Urban-rural differences in drug overdose death rates, 2020. NCHS Data Brief 440

Spencer MR, Miniño AM, Warner M (2022b) Drug overdose deaths in the United States, 2001–2021. NCHS Data Brief 457

Tang J, Scellato S, Musolesi M et al (2010) Small-world behavior in time-varying graphs. Phys Rev E 81(5):055101

Tukey JW (1949) Comparing individual means in the analysis of variance. Biometrics 5:99–114

Turnbull BW (1976) The empirical distribution function with arbitrarily grouped, censored and truncated data. J Roy Stat Soc: Ser B (Methodol) 38(3):290–295

Valente TW, Pitts SR (2017) An appraisal of social network theory and analysis as applied to public health: challenges and opportunities. Annu Rev Public Health 38:103–118

Van Daele S, Vander Beken T (2010) Journey to crime of "itinerant crime groups". Polic: Int J Police Strateg Manag 33(2):339–353

Vandeviver C, Van Daele S, Vander Beken T (2015) What makes long crime trips worth undertaking? Balancing costs and benefits in burglars' journey to crime. Br J Criminol 55(2):399–420

Yang KC, Aronson B, Odabas M et al (2022) Comparing measures of centrality in bipartite patient-prescriber networks: a study of drug seeking for opioid analgesics. PLoS ONE 17(8):e0273569

Publisher's Note